A Remediation Approach to Chromium-Contaminated Water and Soil using Engineered Biochar Derived from Peanut Shell

Published in: *Environmental Research*

Citation for published version: Murad, H.A., Ahmad, M., Bundschuh, J., Hashimoto, Y., Zhang, M., Sarkar, B., Ok, Y.S., (2022) A Remediation Approach to Chromium-Contaminated Water and Soil using Engineered Biochar Derived from Peanut Shell. *Environmental Research*, 204: 112125. doi: 10.1016/j.envres.2021.112125.

Document version: Accepted peer-reviewed version.

A Remediation Approach to Chromium-Contaminated Water and Soil using Engineered Biochar Derived from Peanut Shell

Hafiza Afia Murad[a,1], Mahtab Ahmad[a,1,*], Jochen Bundschuh[b], Yohey Hashimoto[c], Ming Zhang[d], Binoy Sarkar[e], Yong Sik Ok[f,*]

[a] Department of Environmental Sciences, Faculty of Biological Sciences, Quaid-i-Azam University, Islamabad 45320, Pakistan

[b] UNESCO Chair on Groundwater Arsenic within the 2030 Agenda for Sustainable Development, University of Southern Queensland, West Street, Toowoomba, Queensland 4350, Australia

[c] Department of Bio-Applications and Systems Engineering, Tokyo University of Agriculture and Technology, 2-24-16 Koganei, Tokyo 184-8588, Japan

[d] Department of Environmental Engineering, China Jiliang University, No. 258 Xueyuan Street, Hangzhou, Zhejiang 310018, China

[e] Lancaster Environment Center, Lancaster University, Lancaster, LA1 4YQ, United Kingdom

[f] Korea Biochar Research Center, APRU Sustainable Waste Management Program & Division of Environmental Science and Ecological Engineering, Korea University, Seoul, Korea

[1] These authors share co-first authorship.

* Corresponding authors

Email: mahmad@qau.edu.pk (Mahtab Ahmad); yongsikok@korea.ac.kr (Yong Sik Ok)

Highlights

- Peanut shells were converted to biochar, and engineered with CTAB
- High Cr(VI) removal efficiency for the engineered biochar (79.35%) was observed
- Chemisorption was the main mechanism of interaction between Cr(VI) and the biochar
- High immobilization of Cr(VI) was observed in the soil with engineered biochar

Abstract

Hexavalent chromium (Cr[VI]) is one of the major environmental concerns due to its excessive discharge through effluents from the leather tanning industry. Peanut production leads to the generation of residual shells as waste calling for sustainable disposal. In this study, we employed an innovative approach of applying peanut-shell-derived pristine and engineered biochar for the remediation of Cr-contaminated wastewater and soil. The peanut shell waste was converted to biochar, which was further engineered with cetyltrimethylammonium bromide (CTAB, a commonly used cationic surfactant). The biochars were then used for the adsorption and immobilization of Cr(VI) in water and soil, respectively. The adsorption experiments demonstrated high Cr(VI) removal efficiency for the engineered biochar (79.35%) compared with the pristine biochar (37.47%). The Langmuir model best described the Cr(VI) adsorption onto the biochars ($R^2 > 0.97$), indicating monolayer adsorption. Meanwhile, the adsorption kinetics indicated that chemisorption was the dominant mechanism of interaction between the Cr(VI) and the biochars, as indicated by the best fitting to the pseudo-second-order model ($R^2 > 0.98$). Adsorption through the fixed-bed column also presented higher Cr(VI) adsorption onto the engineered biochar (q_{eq} = 22.93 mg g^{-1}) than onto the pristine biochar (q_{eq} = 18.54 mg g^{-1}). In addition, the desorption rate was higher for the pristine biochar column (13.83 mg g^{-1}) than the engineered biochar column (10.45 mg g^{-1}), indicating that Cr(VI) was more strongly adsorbed onto the engineered biochar. A higher immobilization of Cr(VI) was observed in the soil with the engineered biochar than with the pristine biochar, as was confirmed by the significant decreases in the Cr(VI) bioavailability (92%), leachability (100%), and bioaccessibility (97%) compared

with the control (soil without biochar). The CTAB-engineered biochar could thus potentially be used as an efficient adsorbent for the removal and the immobilization of Cr(VI) in water and soil, respectively.

Keywords: Designer biochar; Soil quality; Soil remediation; Sustainable Development Goals; Life on land

1. Introduction

Chromium (Cr), which generally exists in trivalent or hexavalent form, is discharged through the leather tanning, metal processing, mining, and electroplating industries, causing severe contamination to water, soil, and plants worldwide (Rajapaksha et al., 2018). Specifically, the wastewater from leather tanning industry can contain 1,500–3,000 mg L^{-1} Cr (Sabur et al., 2013), and there has been a global increase in Cr concentrations in water bodies pertaining to this industry. High concentrations of up to 84, 50, and 60 µg L^{-1} Cr in surface water, groundwater, and drinking water, respectively, have been reported in major countries around the globe, while the permissible limit is 0.5–2 µg L^{-1} (Jobby et al., 2018). The hexavalent chromium (Cr[VI]) is around 500 times more toxic than trivalent chromium (Cr[III]), and can cause carcinogenesis, teratogenesis, and mutations in living bodies (Chen et al., 2015). In fact, Cr(VI) is included in the United States Environmental Protection Agency's list of top-priority hazardous pollutants (US-EPA, 2014).

Soil is a major sink for heavy metals released into the environment via anthropogenic activities such as the disposal of tannery waste and various activities pertaining to the metallurgy industry. Globally, 896 tons of Cr is disposed of each year into soils (Mohan and Pittman, 2006). Irrigation through metal-contaminated wastewater and sludge application is also causing the contamination of soil and various crops, and their long-term persistence is somewhat alarming (Kumar et al., 2005). Specifically, tannery sludge contains 4.2% of Cr (Xia et al., 2019), largely comprised of extremely mobile fractions, which consequently poses the threat of soil and water contamination in the nearby areas (Riaz et al., 2020). There is thus an urgent need to design cost-effective and simple technology to remove Cr(VI) from the wastewater in water bodies as well as from soil (Palansooriya et al., 2020).

The available techniques for industrial wastewater treatment are adsorption, ion exchange, chemical precipitation, oxidation/reduction, and membrane separation (e.g., reverse osmosis and ultrafiltration) (Wang et al., 2019). Meanwhile, soil washing, immobilization, phytoremediation, soil extraction, and vitrification are among the available treatment technologies for heavy-metal-contaminated soils (Fytianos et al., 2000). The carbon-based adsorbents have been reported as efficient means of remediating the metal-contaminated water and soil (Hilber and Bucheli, 2010; Yang et al., 2019). Biochar, a carbon-rich material obtained from the thermal processing of bio-waste, has recently emerged as a promising adsorbent for wastewater treatment and a promising soil amendment (El-Naggar et al., 2018a).

Bio-waste will ideally produce biochar in such a way that it reduces the waste burden and helps in the area of waste management. In fact, this can lead to achieving sustainable development goals (set by the General Assembly of the United Nations) in terms of good health and well-being (Goal 3), clean water and sanitation (Goal 6), climate action (Goal 13), and life on land (Goal 15) (Kumar and Bhattacharya, 2020). Peanut shells are generated as waste following the peanuts' consumption as food. It is estimated that 1.6 ton ha^{-1} of peanut shell waste is produced worldwide (Torkashvand et al., 2015). Specifically, in Pakistan, 18,280 ton yr^{-1} of peanut shell waste is generated, with the total peanut production amounting to 91,400 ton yr^{-1} (PARC, 2020). The peanut shells are largely burned in the open atmosphere, causing greenhouse gas emissions, or become buried in soil, with a slow degradation rate (Duc et al., 2019). Unlike other biowaste types, peanut shells are not decomposed easily in the environment because of their high lignin contents. Additionally, peanut shells exhibit adsorption potential for heavy metals such as Cu, Ni, Zn, and Cr (Duc et al., 2019). To avoid environmental issues related to peanut shells waste disposal and to synthesize an efficient adsorbent, the material could be a valuable feedstock for biochar production. Various recent studies have reported biochar's efficacy in terms of Cr(VI) removal from water (Rajapaksha et al., 2018; Huang et al., 2020) and Cr(VI) immobilization in soil (Rafique et al., 2020; Khan et al., 2020). However, an innovative and systematic approach of applying peanut-shell-derived biochar for the remediation of Cr-contaminated water and soil has, as yet, not been reported.

A common restraint in the application of pristine biochar is its relatively low efficiency for contaminant mitigation, which has led to the engineering of biochar surfaces to remediate metal-contaminated water and soil (Zhang et al., 2020; Wang et al., 2020). Biochar can be engineered via acid/base, magnetic, steam, amine, or surfactant treatments, depending on the desired properties of the engineered product (Rajapaksha et al., 2016). Specifically, ionic surfactants can easily bind onto the biochar surfaces to facilitate the electrostatic interaction with the ionic contaminants (Saleh, 2006). However, the biochar surface is generally negatively charged ($pH_{PZC} < 7$; Li et al., 2017), which means pristine biochar may not be effective in removing anionic forms of metals (e.g., chromate [CrO_4^{2-}] and dichromate [$Cr_2O_7^{2-}$]) due to electrostatic repulsion. Engineering the biochar with a cationic surfactant may alter the biochar surface from a negative to a positive charge (El-Naggar et al., 2018b). The resulting engineered biochar will have the potential capacity for effectively removing anionic forms of metal such as CrO_4^{2-} (Cr[VI]) from water, while it could also reduce the mobility of Cr(VI) in soil.

Cetyltrimethylammonium bromide (CTAB) is a cationic surfactant that can be used for biochar engineering due to its reported ability to increase the positive charge on the biochar surface (Mathurasa and Damrongsiri, 2017; Li et al., 2018). Moreover, surfactants tend to be commonly used household chemicals, and are thus easily available for biochar engineering purposes. It is hypothesized that the Cr(VI) in its anionic form could be attracted by the positively charged micelles of the CTAB anchored on biochar, which will enable the on-site covalent bonding with Cr(VI). Hence, the present study was aimed at developing an innovative approach to remediating the Cr(VI)-contaminated wastewater and soil impacted by tannery industry using CTAB-engineered biochar derived from peanut shells. Furthermore, we also evaluated the Cr(VI) remediation potentials by comparing the efficacy of pristine and engineered biochars.

2. Materials and methods

2.1. Preparation, engineering, and characterization of biochar

Peanut shells were collected from household waste and university campus residential areas. The feedstock was chopped to a small particle size and subjected to pyrolysis for biochar production. The biochar was produced by pyrolyzing the processed peanut shells in a muffle furnace (Vulcan D-550, USA) under limited oxygen conditions at a heating rate of 6°C min^{-1}. The carbonization process temperature was fixed at 600°C, with the heating continued at this temperature for 2 h. The resulting pristine biochar (PBC) was allowed to cool at room temperature and was then stored in zipper bags to prevent moisture until used.

For the engineering of the biochar, we adopted the chemical modification process reported by Mi et al. (2016). In brief, the biochar was first acid-washed with 4 M HCl solution for 12 h to remove any minerals before being separated via filtration using Whatman 42 filter paper. The filtered biochar was then washed with distilled water several times to achieve a neutral pH before being dried overnight in an oven at 80°C. Following this, the demineralized biochar was added into 1% CTAB solution at a rate of 1% wt/vol. The mixture was then stirred at 700 rpm for 24 h using a magnetic stirrer. The suspension was then filtered through Whatman 42 filter paper to obtain the solid product, which was then oven-dried at 80°C overnight. The final engineered biochar (EBC) product was then stored in an airtight container for further analysis and application.

The produced biochars (PBC and EBC) were subjected to proximate analysis (moisture, mobile matter, resident matter, and ash), as well as pH, electrical conductivity (EC), organic matter, scanning electron microscopy (SEM), and Fourier transform infrared (FTIR) spectroscopy analyses. The proximate and chemical analytical procedures were carried out with reference to Ahmad et al. (2012a). Various SEM images of the biochar surfaces were taken using a JSM-6490A, JEOL (Japan) microscope, while the Spectral 65 Perkin Elmer (USA) FTIR instrument was used for the determination of the functional groups on the biochar surfaces. The pH point of zero charges (pH_{PZC}) of the biochars was determined following the method reported by Xu et al. (2019). Briefly, a 0.1 g biochar sample was stirred in 50 mL of 0.01 M $CaCl_2$ solution, the pH of which was adjusted with values ranging from 2 to 12 (with 0.5 M HCl or NaOH solutions) for 24 h at 120 rpm. The pH_{PZC} was calculated by plotting the ΔpH (difference in final and initial pH) against the initial pH values.

2.2. Wastewater and soil collection, processing, and characterization

Soil and wastewater samples were collected from a tannery industry zone located near Sialkot, Pakistan. The wastewater samples were collected from the disposal point of the industrial zone in pre-cleaned plastic bottles and were subsequently filtered through Whatman 42 filter paper to remove any suspended particles. The soil samples were collected from a radius of 1 km surrounding the industrial zone, with the top 15–20 cm of soil grabbed from different points. A composite sample was then produced by mixing and homogenizing the grab samples in a polythene sack. The samples were preserved either in pre-cleaned plastic bottles or bags at 4°C prior to the laboratory analysis. The soil was air-dried and sieved through a 2-mm aperture to remove any gravel or other rubble and to ensure homogenized soil particles were obtained. The total amount of Cr in the wastewater samples was measured following the acid digestion method (method 3005a; US-EPA 1992a) using an atomic absorption spectrometer (AAS; SpectrAA-220, Varian, USA). The presence of Cr(VI) was determined colorimetrically (method 7196a; US-EPA 1992b) using diphenyl carbazide with a UV-visible spectrophotometer (Bio-Rad UV3000, USA). The total concentrations of Cr and Cr(VI) in the wastewater samples were 40.83 ± 3.52 and 24.86 ± 0.23 mg L^{-1}, respectively. Meanwhile, the soil was characterized in terms of general soil parameters (pH, EC, texture, organic matter, etc.) following the methods reported by Estefan et al. (2013), and total Cr concentration following the acid digestion method (method 3050; US-EPA 1992c) using the AAS. The soil was acidic (pH 5.00 ± 0.02) with a silt loam texture. The total Cr and Cr(VI) concentrations in the soil were 1992.23 ± 19.20 and 212.88 ± 15.06 mg kg^{-1} (see Table S1 in the supplementary material).

2.3. Equilibrium adsorption experiments

The biochars (PBC and EBC) were tested for their adsorption capacities in terms of aqueous Cr(VI) removal. Here, batch-type equilibrium isotherm and kinetics experiments were performed. First, potassium dichromate ($K_2Cr_2O_7$) was used to prepare a stock solution of 500 mg L^{-1} Cr(VI) in deionized water. A series of concentrations, including 5, 10, 25, 50, 150, and 300 mg L^{-1}, were then prepared for the equilibrium adsorption experiments. A relatively high concentration range of Cr(VI) (0–300 mg L^{-1}) was selected due to the high average concentration (~ 400 mg L^{-1}) reported in the wastewater of different local tannery industries in Pakistan (Bhalli and Khan, 2006). For each batch experiment, a 45 mL solution of each concentration was taken in a 50 mL falcon tube, with the biochar dose fixed at a rate of 2 g L^{-1}. Then, the samples were shaken using a horizontal shaker at 110 rpm at room temperature for 24 h. Following this, the solutions were filtered through Whatman 42 filter paper, and the Cr(VI) concentration in the aqueous phase was determined. Control samples (without biochar) were also used for each batch experiment. All experiments were performed in triplicate. The amount of adsorbed contaminant was calculated using the following equation (Volesky, 2007):

$$\mathrm{Q_e} = (\mathrm{C_o} - \mathrm{C_e}) \times \mathrm{v/w}$$

where Q_e is the amount of Cr(VI) (mg g^{-1}) adsorbed by the biochar at equilibrium, C_o is the initial Cr(VI) concentration in the solution, C_e is the remaining concentration in the solution at equilibrium, *v* is the volume of the solution (L), and *w* is the weight of the biochar (g). The Cr(VI) removal efficiency of each biochar was calculated using the following equation:

$$\text{Removal (\%)} = \left(\frac{\mathrm{C_o} - \mathrm{C_e}}{\mathrm{C_o}}\right) \times 100$$

Three isotherm models, the Freundlich, Langmuir, and Temkin models, were employed to optimize the usage efficiency of the biochar. The Freundlich model describes the adsorption on the heterogeneous surface and the multilayer adsorption and is expressed by the following equation (Tran et al., 2017):

$$\mathrm{Q_e} = \mathrm{K_F}\, C_e^N$$

where K_F is the capacity of the adsorbent to sorb the adsorbate (mg g^{-1}) and *N* is the parameter pertaining to the linearity. Meanwhile, the Langmuir model explicates the adsorption on a homogeneous surface and defines the monolayer adsorption on the surface of the adsorbents according to the following equation (Tran et al., 2017):

$$Q_e = Q_{max} K_L C_e (1 + K_L C_e)^{-1}$$

where Q_{max} is the maximum amount of Cr(VI) adsorbed (mg g^{-1}) and K_L is the adsorption equilibrium constant (L mg^{-1}). Finally, the Temkin isotherm model is specifically related to the adsorption heat, providing evidence regarding the effects of any indirect adsorbate/adsorbate connections on the adsorption process. In short, the model assesses how the heat of adsorption of all the molecules in the layer decreases linearly due to the increase in surface coverage, which can be articulated using the following equation (Ahmad et al., 2013a):

$$Q_e = \frac{RT}{B} \ln(A\, C_e)$$

where *R*, *T*, *B*, and *A* are the universal gas constant (8.314 J K^{-1} mol^{-1}), the absolute temperature (273 K), the heat of adsorption (J mol^{-1}), and the binding constant (L mg^{-1}), respectively.

The Chi-squared (χ^2) test was also used to estimate the fitting of the experimental data to the models' predicted values. The following equation was used (Arshadi et al., 2014):

$$\chi^2 = \sum \frac{(Q_e - Q_c)^2}{Q_c}$$

where Q_e and Q_c are the experimental and the model-calculated adsorbed amounts of Cr(VI), respectively.

2.4. Kinetics adsorption experiments

Adsorption kinetics experiments were performed to analyze the adsorption mechanism on the surface of the biochars. Here, an initial concentration of 10 mg L^{-1} Cr(VI) was used, while the biochar dose was fixed at 5 g L^{-1}. A relatively low initial Cr(VI) concentration and a comparatively high biochar dose were used in the kinetics experiments compared with in the equilibrium adsorption experiments to attain maximum adsorption in the given contact time. Samples with three replicates were placed on a horizontal shaker at 110 rpm, with samples taken at nine different time intervals of 15 min, 30 min, 1 h, 2 h, 3 h, 5 h, 10 h, 24 h, and 48 h. Following this, the samples were filtered through Whatman 42 filter paper and analyzed in terms of Cr(VI) using the UV-visible spectrophotometer. Different models, including first-order, second-order, pseudo-second-order, and intra-particle diffusion models were applied to the kinetics experimental data. The equations of the different models are given below (Ahmad et al., 2013b):

First-order: $\ln q_t = \ln q_o - k_1 t$

Second-order: $\frac{1}{q_t} = \frac{1}{q_o}\ k_2 t$

Pseudo-second-order: $\frac{t}{q_t} = \left(\frac{1}{k_2^{`}}\ q_e^2\right) + \frac{t}{q_e}$

Intra-particle diffusion: $q_t = C + K_d\ t^{0.5}$

where q_t and q_o are the adsorption capacities (mg g^{-1}) at time *t* and 0, respectively, k_1, $k_{2,}$ and k_2´ are the rate constants of the first-, second-, and pseudo-second-order models, respectively, q_e (mg g^{-1}) refers to the adsorption capacity when an equilibrium is established, *C* is the diffusion rate constant ([mg $g^{-1}]^{-0.5}$), and K_d is the diffusion constant.

2.5. Continuous fixed-bed column adsorption and desorption experiments

For the column adsorption experiments, polyacrylic columns 9.4-cm in length and 2-cm in inner diameter were used. A 7-g sample of each biochar (PBC and EBC) was placed in the polyacrylic columns. The real wastewater of the tannery industry was passed as an influent through the column from the top at a rate of 6 mL min^{-1}. The empty bed contact time of the column was 2.83 min. The effluent from each column was collected from the outlet of the column at different time intervals (0.5, 1, 2, 3, 4, 6, 8, 10, 12, 14, 16, 20, and 24 h), and was analyzed in terms of Cr(VI) using the UV-visible spectrophotometer. As such, the effluent samples were continuously analyzed in terms of Cr(VI) until the concentration became almost equal to the concentration of Cr(VI) in the real wastewater. After exhausting the column with Cr(VI), the saturated sorbents were eluted with 0.1 N HNO_3 at a flow rate of 6 mL min^{-1}.

For the calculations of the adsorption and desorption parameters in the continuous fixed-bed biochar columns, the methods reported by Zhang et al. (2015) were followed. Details of the column data analysis for the adsorption and desorption of Cr(VI) are provided in the supplementary material. The behavior of Cr(VI) adsorption on the two biochars was evaluated by subjecting the experimental column adsorption data to the Thomas model, which is given by the following equation (Hanbali et al., 2014):

$$\ln\left[\frac{C_o}{C_e} - 1\right] = \frac{k}{Q}\left[q_m X - C_o V_{ef}\right]$$

where k is the rate constant (mL min^{-1} mg^{-1}), q_m is the maximum amount of Cr(VI) adsorbed (mg g^{-1}), X is the weight of the sorbent (g), and V_{ef} is the effluent volume (mL). The elution efficiency (E) of each column was calculated using the following equation:

$$E\ (\%) = \left[\frac{q_{total(desorbed)}}{q_{total(sorbed)}}\right] \times 100$$

where $q_{total(desorbed)}$ (mg g^{-1}) was calculated from the area under the elution curve.

2.6. Soil remediation experiment

The biochars (PBC and EBC) were evaluated in terms of their remediation potential in Cr-contaminated soil of a specific tannery industry. A soil incubation experiment was conducted using three applications (1%, 2%, and 5% w/w) of each biochar. Specifically, Cr-contaminated soil (200 g) samples were taken in each polyethylene container (300-mL capacity) and then mixed with the above-mentioned application rates for each biochar type. The soil was wetted with 35 mL of distilled water according to 55% of the soil water-holding capacity. The experiment was conducted in triplicates. Controls (soil without biochar) were also treated in the same manner. The soil moisture was sustained with distilled water repeatedly throughout the experiment by weighing each container periodically. The containers were tightly closed and incubated in the dark at room temperature, with the incubation experiment carried out over 45 days. Following the incubation, the soil samples of each treatment were air-dried and subjected to various extraction tests to investigate the bioavailability, leachability, and bioaccessibility of the Cr(VI). The bioavailable Cr(VI) was measured in a 1:10 soil water extract, while for the toxicity characteristics, the toxicity characteristics leaching procedure (TCLP) method 1311 (US-EPA, 1992d) was adopted to determine the leachability, with the bioaccessibility of the Cr(VI) determined following the physiologically based extraction test (PBET) (Ahmad et al., 2012a). In each extraction test, the filtered extract (using Whatman 42 filter paper) was analyzed in terms of Cr(VI) via a colorimetric method (as noted earlier).

Water-soluble NO_3 and PO_4 (in addition to pH and EC) were also measured in the incubated soils (1:10 soil water extract) following the colorimetric method while using phenol disulfonic acid and ammonium molybdate reagents, respectively, with the UV-visible spectrophotometer at 410 and 690 nm, respectively (Trivedy et al., 1987).

2.7. Statistical analysis

The mean values of the three replicates were used to plot isotherms for the equilibrium and kinetic adsorption experiments. Linear and non-linear regressions were carried out in SigmaPlot (version 10.0) for fitting the adsorption experimental data to various models. Meanwhile, one way analysis of variance was applied in combination with Tukey's honestly significant difference test to determine the significant differences between the different treatments.

3. Results and discussion

3.1. Biochar properties

The results of the proximate and physicochemical analyses of the PBC and the EBC are presented in Table S2 (supplementary material). The mobile matter in the PBC, which indicates the biodegradable content, was 24.11% ± 0.56%, which was decreased significantly to 20.15% ± 0.35% in the EBC due to the loss during the engineering process resulting from, for example, the demineralization with acid (section 2.1; Vithanage et al., 2015). The ash content in the biochar samples was relatively high (>55%), which could have been due to the accumulation of inorganic minerals present in the feedstock during the process of pyrolysis (Ahmad et al., 2014). The PBC was highly alkaline with a pH value of 9.46 ± 0.01, while the EBC was slightly acidic with a pH value of 6.30 ± 0.01. The alkaline nature of the PBC was due to the existence of alkali salts and the removal of the acidic functional groups during pyrolysis at 600°C. Meanwhile, the acid demineralization and washing processes during the biochar engineering resulted in the acidic nature of the EBC. These results were consistent with the EC values of the biochars, where the PBC had a higher EC (0.249 ± 0.007 dS m^{-1}) than the EBC (0.149 ± 0.002 dS m^{-1}). Here, the biochar engineering eliminated one of the limitations of applying alkaline biochars to normal or alkaline soils, as demonstrated by the EBC, which exhibited an acidic pH. The pH_{PZC} of the PBC and EBC was 7.44 ± 0.07 and 6.70 ± 0.04, respectively, indicating that with any pH lower than this in an aqueous solution, the biochar surfaces will be positively charged, and vice versa. The organic matter in the PBC (1.66% ± 0.33%) was significantly greater than that in the EBC (1.15% ± 0.34%), which was again due to the demineralization step involved in the engineering process.

The surface morphological structures of the biochars were visualized using SEM images (Fig. 1). Here, the typical plant morphological structure with various pores and channels could be observed in the PBC. However, the surface structure of the EBC was different from that of the PBC. Here, a relatively smooth surface with diffused pores was observed in the EBC, which was likely due to the engineering with CTAB. A pore blockage and a decrease in surface area of biochars following CTAB modification have been previously reported (Liu et al., 2020).

The changes in the surface chemistry of the biochars following engineering were analyzed using the FTIR spectra (Fig. 2), with the spectra interpreted following the information provided by Coates (2000), Keiluweit et al. (2010), and Li et al. (2018). The FTIR results indicated clear differences in the surface functional groups of the PBC and the EBC. In the former, the absorbance bands at 1,570, 1,390, 1,024, and 871 cm^{-1} indicated the presence of C=C-C, CH_2, aromatic C-N, and aromatic C-H stretch, respectively. Specifically, the aromatic C-N and CH out of plane bending vibrations suggested the development of a stable aromatic structure of the PBC, which was due to the pyrolysis at 600°C. Meanwhile, more diverse and intense functional groups were observed in the EBC, which was due to the engineering with CTAB. Specific bands of the CTAB material were present on the surfaces of the EBC, demonstrating the effect of modification on the biochar's surface chemistry. The broad band at 3,290 cm^{-1} indicated the presence of NH_4^+ ion in the EBC, while the bands at 2,970–2,850, 1,600–1,750, 1,465, 1,280, and 1,210 cm^{-1} indicated the typical presence of C-H stretch, carbonyl groups, N-CH_3, aromatic ether, and C-N groups, respectively. Meanwhile, the bands at 990–1,100, 890, and 700 cm^{-1} indicated the presence of P-O-C, Si-O-C, aromatic C-H stretch, and C-Br, respectively. These results suggested the more complex surface chemistry of the EBC compared with the PBC.

The effect of the engineering process on the biochar properties could further influence their applicability. In short, the appearance of positively charged ions (e.g., NH_4^+) on the EBC could facilitate the adsorption of Cr(VI). Likewise, more acidic functional groups (carbonyl, N- and P-containing functional groups) on the EBC may contribute to the better removal of anionic Cr(VI) compared with the PBC.

3.2. Removal of hexavalent chromium from water

3.2.1. Effect of initial hexavalent chromium concentration and contact time

With an increase in initial Cr(VI) concentration (from 5 to 300 mg L^{-1}) the removal efficiency of both the biochars decreased (see Fig. S1a in the supplementary material). This could be due to the occupation of active sites on the biochar surfaces by the Cr(VI). At high initial Cr(VI) concentrations, fewer active sites were available to adsorb high contents of Cr(VI). Between the two biochars, the EBC demonstrated a greater removal efficiency than the PBC. For example, the highest removal efficiency of 79.35% was observed at a 5-mg L^{-1} concentration of Cr(VI) with the EBC, while at the same initial concentration, the PBC demonstrated only a 37.47% removal. These results indicated that the CTAB engineering may have increased the number of positively charged active sites on the EBC surface, which subsequently contributed to its higher removal efficiency compared with that of the PBC. The decrease in removal efficiency with the elevation in initial metal ion content is a general phenomenon that occurs when testing an adsorbent for its adsorption capacity (Wadhawan et al., 2020).

The contact time between sorbent and sorbate determines the rate of a chemical reaction. Greater adsorption in a lower time of contact indicates rapid reaction and vice versa. In this study, the results indicated clear differences between the two biochars in terms of Cr(VI)-removal efficiency, with the EBC demonstrating greater removal efficiency than the PBC at all contact times. In fact, in the case of the EBC, the Cr(VI) removal increased from 47.58% to 54.33% within 1.0 h of contact time, followed by a decrease to 48.99% for 3.0 h and then a gradual increase up to 72.37% after 48 h of contact time. Likewise, there was no sharp increase in Cr(VI) removal up to 5 h of contact time in the case of the PBC; however, after this point, there was a gradual increase in Cr(VI) removal up to 42.59% after 48 h of contact time. These results suggest that both biochars required a longer contact time for the maximum removal of Cr(VI) from water. This could have been due to the persistence of the natural composition of the feedstock and the limited availability of active sites, particularly in the case of the PBC. Furthermore, the functional groups on biochars tend to become stabilized in forming complexes with Cr(VI), thereby lowering the adsorption efficiency with the increase in contact time (Lian et al., 2019). The pH_{PZC} is another important parameter for determining the charge on biochar surfaces. After 5 h of contact time, the solution pH was lower than the pH_{PZC} of both biochars (solution pH 6.04 < 7.44 pH_{PZC} of PBC, and solution pH 6.20 < 6.70 pH_{PZC} of

EBC), indicating that, at this point, the biochar surfaces were positively charged, which resulted in the electrostatic attraction of negative ionic species of Cr(VI) ($Cr_2O_7^{2-}$ and $HCrO_4^-$). However, the biochar surfaces became negatively charged at and beyond 24 h of contact time when the solution pH was > 8, thus causing a slow adsorption rate due to the lack of electrostatic attraction. Nevertheless, the biochar engineering resulted in comparatively high Cr(VI) removal rates at various time intervals in comparison with the non-engineered biochar. These results are consistent with those reported by Li et al. (2018), who described how hydrophilic and hydrophobic functional groups on their CTAB-modified biochar increased its adsorption efficiency in comparison with the pristine biochar. In the current study, the EBC was loaded with more aromatic functional groups than the PBC (Fig. 2), which facilitated the greater removal of the Cr(VI).

3.2.2. Adsorption isotherms

The Langmuir, Freundlich, and Temkin isotherm models were fitted through non-linear regressions to the Cr(VI) adsorption data of the biochars, with the fitting results shown in Fig. 3. Meanwhile, the constant parameters and R^2 values of the different models for Cr(VI) adsorption onto the different biochars were obtained and are provided in Table 1a. Here, the R^2 values of the Langmuir model for the PBC and the EBC were 0.998 and 0.978, respectively, while the corresponding χ^2 values were 0.073 and 0.700, respectively. The Langmuir model predicted a maximum adsorption capacity (Q_{max}) of 14.56 mg g^{-1} for the PBC and 27.05 mg g^{-1} for the EBC. The good fitting of the adsorption data to the Langmuir model indicated that Cr(VI) may have adsorbed onto the biochar monolayers. Meanwhile, in the Freundlich isotherm model, the R^2 values were 0.986 and 0.964 for the PBC and the EBC, respectively, while the corresponding χ^2 values were 0.423 and 1.196, respectively. The constant K_F is an approximate indicator of adsorption capacity, while N is a function of the strength of adsorption in the adsorption process. If the value of N is below 1, it indicates normal adsorption, while a value of above 1 indicates cooperative adsorption (Puttamat and Pavarajarn, 2016). Here, the N values for both biochars were <1, indicating that there was no cooperative adsorption, while the K_F value for the EBC (0.491 mg g^{-1}) was significantly higher than that for the PBC

(0.194 mg g^{-1}), indicating a similar trend to that of the Langmuir model. Finally, in the Temkin isotherm model, the R^2 values were 0.914 and 0.818 for the PBC and the EBC, respectively, while the corresponding χ^2 values were 0.022 and 0.016, respectively. The model-calculated *B* value was lower for the EBC (371.1) than for the PBC (577.5), indicating the greater adsorption of Cr(VI) onto the EBC due to a decrease in the adsorption heat and a uniform sharing of the binding energies.

Based on the R^2 and χ^2 values, the Langmuir model was better fitted to our experimental data than the other models. Somewhat, the EBC demonstrated greater adsorption of Cr(VI) than the PBC, as was predicted by all three models. It is notable that due to the multivariate properties of biochar, several adsorption mechanisms could be involved in the elimination of Cr(VI) from water. In this study, the overall controlling mechanism of adsorption could be the monolayer-to-multilayer adsorption of Cr(VI) onto the biochar surface, as indicated by the good fit of the adsorption data to both the Langmuir model and the Freundlich model.

3.2.3. Adsorption kinetics

Adsorption kinetics experiments are generally performed to determine the rate of adsorption, including in terms of mass transport and chemical reaction processes. Here, the adsorption kinetics data were fitted linearly to various kinetic models (first-order, second-order, pseudo-second-order, and intra-particle diffusion), as shown in Fig. 4. The calculated constant parameters and R^2 values of the different kinetics models are given in Table 1b. The pseudo-second-order model exhibited high R^2 values for both the PBC (0.985) and the EBC (0.996). This model explains that the mechanism of interaction between adsorbent and adsorbate could be via chemical bonding or via complexation involving electron exchange, which is generally known as chemisorption. Between the two biochars, the EBC exhibited a greater q_e of 0.851 mg g^{-1} than the PBC (0.497 mg g^{-1}), as predicted by the pseudo-second-order model. Similarly, a higher rate of reaction (k_2') was exhibited by the EBC (1.088 g mg^{-1} h^{-1}) than the PBC (1.020 g mg^{-1} h^{-1}), indicating that the adsorption kinetics of aqueous Cr(VI) occurred faster in the former than in the latter. The other kinetic models were poorly fitted to the Cr(VI) adsorption data, as indicated by the R^2 values of <0.9. These results indicate that chemisorption could be the main mechanism for aqueous Cr(VI) removal by biochars. The kinetics analysis also confirmed that the EBC was a more efficient sorbent in removing Cr(VI) from water.

The adsorption experiments indicated the comparatively greater efficiency of the EBC than the PBC. This could have been due to the changes in biochar properties following the CTAB engineering. For example, more aromatic and positively charged functional groups were observed on the EBC than on the PBC (Fig. 2), which could have been involved in complex formation with the Cr(VI). Moreover, the electrostatic interaction between the highly charged surfaces of the EBC and the Cr(VI) could have resulted in the greater adsorption efficiency. In fact, the potential role of surface charge in the adsorption of anionic contaminants with CTAB-modified biochars has previously been reported (Aroke et al., 2014; Mathurasa and Damrongsiri, 2018).

3.2.4. Column adsorption and desorption

The continuous flow fixed-bed columns packed with each PBC and EBC were used for the treatment of real wastewater contaminated with Cr(VI). The adsorbed amount (C_{ad}) of Cr(VI) onto the PBC and EBC columns as a function of time is shown in Fig. S2a (supplementary material). It was observed that up to 4 h, the C_{ad} increased gradually, while after this point, the adsorbed amount became almost constant. This could indicate the equilibrium in Cr(VI) adsorption over time. The saturation time of the fixed-bed column was relatively short, which could be due to the high flow rate of 6.0 mL min^{-1} through the bed of only 6.3 cm height. One of the challenges faced by the column adsorption experiments is the movement of the mass transfer zone, which is initially saturated with the adsorbate molecules near the bed entrance, and further restricts the contact of adsorbent with adsorbate, consequently requiring the replacement of the adsorbent (Patel, 2019). However, as mentioned earlier, this issue can be solved by increasing the bed height of the column, and increasing the contact time, or decreasing the flow rate of influent into the column. Much like with the batch adsorption experiments, the EBC demonstrated greater adsorption of Cr(VI) than the PBC. The performance of the fixed-bed biochar columns in terms of Cr(VI) adsorption was evaluated using the removal percentage of Cr(VI) and the adsorbed amount (q_{eq}) onto the biochars in the columns, with the results presented in Table 2a. The removal efficiencies of the PBC and EBC columns were 60.42% and 74.72%, respectively, while the q_{eq} values were 18.54 mg/g^{-1} and 22.93 mg/g^{-1}, respectively. These results indicated the greater adsorption efficiency of the column packed with the EBC, and were highly consistent with those of the batch adsorption experiments. The Thomas model parameters and R^2 values are shown in Table 2b, with the R^2 values found to be 0.462 and 0.667 for the PBC and the EBC, respectively, which indicated the poor fitting of the column adsorption data to this model. The relatively good fitting of the Cr(VI) adsorption data for the EBC column to the Thomas model indicated that the adsorption was mainly through the mass transfer of Cr(VI) onto the EBC. In this study, Cr(VI) was not removed up to 100%, and the discharge limit of 1.0 mg L^{-1} of Cr(VI) in industrial effluent was not achieved, both in the batch and column adsorption experiments. This could be related to the maximum adsorption potential of the PBC (14.56 mg g^{-1}) and EBC (27.05 mg g^{-1}), which restricted the maximum removal of Cr(VI) to around 79%. However, the removal efficiency can be increased by increasing the amount of adsorbent or bed height of the column, and increasing the contact time, or decreasing the flow rate of the influent into the column. Moreover, for practical application, series of fixed-bed adsorption columns can be employed (Patel, 2019). Once the fixed-bed columns of the PBC and EBC were saturated with Cr(VI), they were eluted with 0.1 M HNO_3 to desorb the Cr(VI) for the separate measurement of the recovery rate of the PBC and the EBC. Figure S2b (supplementary material) shows the desorbed concentrations of Cr(VI) from the saturated PBC and EBC columns at different time intervals. Here, it was observed that at the beginning of the desorption experiment, the desorbed concentration of Cr(VI) was high in the PBC (20.85 mg L^{-1}) and EBC (11.19 mg L^{-1}) columns. The high desorption rate at an initial time, regardless of biochar type, was clear, which was due to the release of loosely bound Cr(VI) from the biochar surfaces. It was also noted that, initially, the desorption rate was higher for the PBC column than for the EBC column, indicating that Cr(VI) was more tightly sorbed onto the EBC. This may suggest some type of strong inner-sphere surface complexation between the Cr(VI) and the EBC. The total time required for the desorption of Cr(VI) from the columns was 40 h for the PBC and 44 h for the EBC. In addition, the fitting of the regression lines indicated a more gradual Cr(VI) desorption from the EBC column (R^2 = 0.931) than from the PBC column (R^2 = 0.813). The desorbed amount of Cr(VI) and the column elution efficiency for the PBC and EBC are shown in Table 2b. The total amount of Cr(VI) desorbed from the PBC and EBC packed columns was 13.83 mg g^{-1} and 10.45 mg g^{-1}, respectively, with an elution efficiency of 74.61% and 45.56% for the PBC and EBC columns, respectively. The greater elution efficiency of the PBC suggested that (i) the Cr(VI) was relatively loosely adsorbed onto the PBC, and (ii) the sorbent could be recycled with greater efficiency after desorbing Cr(VI). Meanwhile, the comparatively lower elution efficiency of the EBC column suggested that (i) the Cr(VI) was relatively strongly sorbed onto the EBC, and that (ii) the Cr(VI) adsorption reaction by the EBC was largely irreversible and that the metal could be retained stably by the EBC. The desorption results indicated that for the removal of Cr(VI) from wastewater, the PBC could be a good candidate, since it can be reused in several cycles for this type of removal.

A few studies have used peanut-shell-derived biochar, albeit engineered with materials other than CTAB, for the removal of aqueous Cr(VI). For example, Al-Othman et al. (2012) reported a 16.26 mg g^{-1} adsorption capacity of KOH-activated carbon derived from peanut shells, while Wang et al. (2020) reported a 15.58 mg g^{-1} adsorption capacity (at 20°C) of kaolinite-modified biochar derived from the same waste product. Overall, the adsorption performance of the CTAB-engineered biochar in this study in terms of aqueous Cr(VI) removal (27.05 mg g^{-1}) was better than those reported in the previous studies.

3.3. Immobilization of hexavalent chromium in soil

The Cr-contaminated soil was treated with different application rates of the two biochars in an incubation experiment. The impact of the biochars on the immobilization of Cr(VI) was evaluated by determining the bioavailable, leachable, and bio-accessible forms of Cr(VI), with the results shown in Fig. 5.

The water-soluble fraction of metals is considered to be the most bioavailable form in soil, one that is readily available for plant uptake. Here, the biochar treatments significantly decreased the water-soluble Cr(VI) content compared with that in the control (Fig. 5a). Specifically, at 1%, 2% and 5% (wt/wt) of the PBC application rates, the water-soluble Cr(VI) decreased from 40.65 mg kg^{-1} (in control soil) to 28.86, 23.52, and 13.33 mg kg^{-1}, respectively. Meanwhile, at 1%, 2% and 5% (wt/wt) applications, the EBC decreased the water-soluble Cr(VI) content to 20.28, 8.14, and 3.35 mg kg^{-1}, respectively. These results indicated the enhanced immobilization of Cr(VI) in the soil with an increase in biochar application rate. On comparing the two biochars at the respective applications, the EBC demonstrated a greater decrease in bioavailability of Cr(VI) (up to 91.75%) in the soil. The possible reason for the greater immobilization efficiency of EBC was related to the reduction of Cr(VI) through the carbonyl functional groups acting as proton donors (Mandal et al., 2017).

The TCLP test is recommended for determining the toxicity of metals in soil, particularly in terms of metals leaching from the soil to the groundwater as a result of acid rain. The control soil with no biochar exhibited high TCLP Cr(VI) content (101.74 mg kg^{-1}; Fig. 5b), indicating that the soil was highly susceptible to Cr(VI) leaching into the groundwater, ultimately causing toxicity. The greater TCLP Cr(VI) content in relation to water-soluble Cr(VI) was due to the acidic extractant (acetic acid) used in the TCLP test. The leachability of Cr(VI) was significantly decreased by the biochars at different applications. Meanwhile, the increase in biochar application resulted in an increase in the immobilization of Cr(VI) in the soil, which could ultimately decrease the toxicity of groundwater. Much like the bioavailable Cr(VI), the leachable Cr(VI) fraction was reduced at a greater rate by the EBC (up to 100%) than the PBC (up to 82.01%). These results suggest that the binding interaction of the EBC in terms of Cr(VI) was greater than that of the PBC.

To ascertain the impact of biochars on the direct ingestion of Cr(VI)-contaminated soil by mammals, a PBET test was performed. This test is useful for determining the toxicity of metals during soil ingestion in the stomach of mammals since the extractant used is highly acidic and is thus representative of actual stomach conditions. The results of the PBET test for Cr(VI) concentration in the contaminated soil treated with the biochars are shown in Fig. 5c. Here, the control soil with no biochar exhibited the highest PBET Cr(VI) concentration (168.97 mg kg^{-1}), which was likely due to the high acidic conditions employed in the PBET test. Both the biochars achieved a significant decrease in the bioaccessibility of Cr(VI), while an increase in biochar application resulted in a greater decrease in the bio-accessible fraction of Cr(VI). Between the two biochars, the EBC again demonstrated a greater immobilization of Cr(VI) (up to 97.26%)

in soil than the PBC (up to 73.32%). These results are consistent with the bioavailable and leachable fractions of Cr(VI).

Overall, in terms of the remediation of Cr-contaminated soil, both biochars were effective in immobilizing the Cr(VI), thereby decreasing its potential to cause toxicity. The greater immobilization effect of the EBC than the PBC indicated that a strong chemical interaction between the Cr(VI) and the EBC surface could have been present. The Cr(VI) remediation in contaminated soil was in good agreement with the results for the Cr(VI) removal from water. Compared with the few available studies on Cr(VI) immobilization in soil using modified biochars, we reported a good efficiency of the EBC. For example, Zibaei et al. (2020) reported 46.23% and 38.95% reductions of Cr(VI) in soil with chitosan-modified and hematite-modified biochars, respectively, while Mandal et al. (2017) reported 55% and 48% reductions in Cr(VI) with chitosan + zerovalent iron-modified sheep manure and poultry-manure-derived biochars, respectively, and Wang et al. (2019) observed a 67.34% decrease in the bioavailability of Cr(VI) in soil treated with bacteria-modified biochar.

Other soil parameters, such as pH, EC, soluble-NO_3, and PO_4, were also analyzed to evaluate the effect of biochars on soil quality, with the results shown in Fig. S3 (supplementary material). A significant increase in the pH was observed for the soils amended with the biochars (Fig. S3a). However, the soil pH was <8, indicating no harmful impact of the biochars since plants can grow normally in such soil types (Soti et al., 2015). A significant decrease in the EC value of the soil was observed in all the biochar applications in relation to the control (Fig. S3b). The reason for this decrease in soil EC could be attributed to the retention of dissolved ions (e.g., Ca^{2+}) on the empty exchange sites of the biochar (Sultan et al., 2020). Specifically, the 5% application of the EBC significantly decreased the soil EC (0.02 dS m^{-1}), which could have been due to its higher adsorption efficiency in terms of soluble ions than the PBC (0.07 dS m^{-1}), as was ascertained from the adsorption experiments. Meanwhile, the soils amended with the PBC exhibited a considerable decrease in the water-soluble NO_3 and PO_4 concentrations (Fig. S3c, d), with the increased application of PBC demonstrating the maximum NO_3 and PO_4 adsorption. In fact, the NO_3 and PO_4 adsorption onto biochars has previously been reported (Zhou et al., 2019). In contrast, the EBC exhibited a significant increase in the NO_3 and PO_4 concentrations (especially at 1% and 2% applications) compared with the control. This could be attributed to the N- and P-containing functional groups present on the EBC surfaces (Fig. 2). From these results, it can be inferred that the EBC could enhance the soil fertility by increasing the bioavailable NO_3 and PO_4 contents in the soil, subsequently improving the plant's growth if the soil is used for agricultural purposes.

Given the better performance of engineered biochar than its pristine counterpart in remediating Cr-contaminated water and soil, and given the additional engineering steps required, the cost of this novel approach could be high (not calculated in this study). However, the benefits of the engineered biochar in comparison with the pristine biochar in terms of higher remediation efficiency could make it an attractive approach in the future. In short, we can design biochars in accordance with the desired application through engineering to avoid any negative impact. Furthermore, using cheap alternative resources, such as household commodities and waste, for the production of engineered biochar could reduce the cost of the attendant technology and subsequently increase the economic profitability.

4. Conclusions

The equilibrium adsorption isotherm experiments indicated a greater adsorption capacity of the engineered biochar (modified with CTAB) than the pristine biochar (derived from peanut shell). The Langmuir model adequately described the adsorption of Cr(VI) onto the biochars, indicating a monolayer type adsorption process. The application of specific kinetic models indicated that chemisorption was the dominant mechanism governing the interaction of Cr(VI) with the pristine and engineered biochars. Similarly, Cr(VI) adsorption decreased gradually through continuous flow fixed-bed columns packed with the pristine and engineered biochars, while the column desorption experiments indicated that Cr(VI) was more tightly adsorbed onto the engineered biochar, suggesting a strong inner-sphere complexation between Cr(VI) and this biochar. To meet the standard discharge limit (1.0 mg L^{-1}) of Cr(VI) from industrial effluents, it is recommended to consider increased bed height, slow flow rate, and series of fixed-bed columns. Both the biochars also demonstrated a great reduction in the bioavailability, leachability, and bioaccessibility of

Cr(IV) in soil. Much like with the water remediation, the engineered biochar was more effective in immobilizing Cr(VI) in the soil. Furthermore, the engineered biochar increased the water-soluble nitrate and phosphate in the amended soil in comparison with the unamended soil, indicating that the remediated soil could be utilized for agricultural purposes. For future research, we suggest employing other engineering processes such as impregnation/coating with chemicals to increase the positive surface charge on biochar for more efficient removal of Cr(VI) from tannery wastewater. Before practical application of the new adsorption technology, the associated factors affecting the removal efficiency, and the permissible discharge limit of the pollutant should be considered.

Acknowledgment

The study was partly supported by the University Research Fund (URF).

References

Ahmad, M., Lee, S.S., Dou, X., Mohan, D., Sung, J.K., Yang, J.E., Ok, Y.S., 2012a Effects of pyrolysis temperature on soybean stover- and peanut shell-derived biochar properties and TCE adsorption in water. Bioresour. Technol., 118, 536-544.

Ahmad, M., Lee, S.S., Yang, J.E., Ro, H.M., Lee, Y.H., Ok, Y.S., 2012b Effects of soil dilution and amendments (musselshell, cowbone, and biochar) on Pb availability and phytotoxicity in military shooting range soil. Ecotoxicol. Environ. Saf., 79, 225-231.

Ahmad, M., Lee, S.S., Rajapaksha, A.U., Vithanage, M., Zhang, M., Cho, J.K., Lee, S.E., Ok, Y.S., 2013a Trichloroethylene adsorption by pine needle biochars produced at various pyrolysis temperatures. Bioresour. Technol., 143, 615-622.

Ahmad, M., Lee, S.S., Oh, S.E., Mohan, D., Moon, D.H., Lee, Y.H., Ok, Y.S., 2013b Modeling adsorption kinetics of trichloroethylene onto biochars derived from soybean stover and peanut shell wastes. Environ. Sci. Pollut. Res., 20, 8364-8373.

Ahmad, M., Rajapaksha, A.U., Lim, J.E., Zhang, M., Bolan, N., Mohan, D., Vithanage, M., Lee, S.S., Ok, Y.S., 2014 Biochar as a sorbent for contaminant management in soil and water: A review. Chemosphere, 99, 19-33.

Al-Othman, Z.A., Ali, R., Naushad, M., 2012 Hexavalent chromium removal from aqueous medium by activated carbon prepared from peanut shell: Adsorption kinetics, equilibrium and thermodynamic studies. Chem. Eng. J., 184, 238-247.

Aroke, U.O., El-Nafaty, U.A., Osha, O.A., 2014 Removal of oxyanion contaminants from wastewater by sorption on to HDTMA Br surface modified organo kaolinite clay. Int. J. Emerging Technol. Adv. Eng., 4, 475-484.

Arshadi, M., Amiri, M.J., Mousavi, S., 2014 Kinetic, equilibrium and thermodynamic investigations of Ni(II), Cd(II), Cu(II) and Co(II) adsorption on barley straw ash. Water Resour. Ind., 6, 1-17.

Bhalli, J.A., Khan, Q.M., 2006 Pollution level analysis in tannery effluents collected from three different cities of Punjab, Pakistan. Pak. J. Biol. Sci., 9, 418-421.

Chilton, P.J., Jamieson, D., Abid, M.S., Milne, C.J., Ince, M.E., Aziz, J.A., 2001 Pakistan water quality mapping and management project. Pakistan Integrated Household Survey (PIHS) Islamabad, Federal Bureau of Statistics, Government of Pakistan.

Coates, J., 2000 Interpretation of Infrared Spectra, a Practical Approach. In: Meyers, R.A. (Ed.), Encyclopedia of Analytical Chemistry. John Wiley & Sons Ltd, Chichester, pp. 10815–10837.

Duc, P.A., Dharanipriya, P., Velmurugan, B.K., Shanmugavadivu, M., 2019 Groundnut shell -a beneficial bio-waste. Biocatal. Agric. Biotechnol., 20, 101206.

El-Naggar, A., Shaheen, S.M., Ok, Y.S., Rinklebe, J., 2018a Biochar affects the dissolved and colloidal concentrations of Cd, Cu, Ni, and Zn and their phytoavailability and potentialmobility in a mining soil under dynamic redox-conditions. Sci. Total Environ., 624, 1059-1071.

El-Naggar, A., Lee, S.S., Awad, Y.M., Yang, X., Ryu, C., Rizwan, M., Rinklebe, J., Tsang, D.C.W., Ok, Y.S., 2018b Influence of soil properties and feedstocks on biochar potential for carbon mineralization and improvement of infertile soils. Geoderma, 332, 100-108.

Estefan, G., Sommer, R., Ryan, J., 2013 Methods of Soil, Plant, and Water Analysis: A manual for the West Asia and North Africa region. 3rd ed. ICARDA (International Center for Agricultural Research in the Dry Areas) Box 114/5055, Beirut, Lebanon, pp. 243.

Fytianos, K., Voudrias, E., Kokkalis, E., 2000 Sorption–desorption behaviour of 2, 4-dichlorophenol by marine sediments. Chemosphere, 40, 3-6.

Hanbali, M., Holail, H., Hammud, H., 2014 Remediation of lead by pretreated red algae: adsorption isotherm, kinetic, column modeling and simulation studies. Green Chem. Lett. Rev., 7, 342-358.

Hilber, I., Bucheli, T.D., 2010 Activated carbon amendment to remediate contaminated sediments and soils: A review. Global Nest J., 12, 305-317.

Huang, S.W., Chen, X., Wang, D.D., Jia, H.L., Wu, L., 2020 Bio-reduction and synchronous removal of hexavalent chromium from aqueous solutions using novel microbial cell/algal-derived biochar particles: Turning an environmental problem into an opportunity. Bioresour. Technol., 309, 123304.

Jobby, R., Jha, P., Yadav, A.K., Desai, N. 2018 Biosorption and biotransformation of hexavalent chromium [Cr(VI)]: A comprehensive review. Chemosphere 207, 255-266.

Keiluweit, M., Nico, P.S., Johnson, M.G., Kleber, M., 2010 Dynamic molecular structure of plant biomass-derived black carbon (biochar). Environ. Sci. Technol., 44, 1247-1253.

Khan, A.Z., Khan, S., Ayaz, T., Brusseau, M.L., Khan, M.A., Nawab, J., Muhammad, S., 2020 Popular wood and sugarcane bagasse biochars reduced uptake of chromium and lead by lettuce from mine-contaminated soil. Environ. Pollut., 263, 114446.

Kumar, A., Bhattacharya, T., 2020 Biochar: a sustainable solution. Environ. Dev. Sustain., https://doi.org/10.1007/s10668-020-00970-0

Kumar, R., Devanathan, A., Rai, A.K., 2015 Speciation of Cr(III) and Cr(VI) in industrial wastewater using biphasic extraction and determination by LIBS. J. Found. Appl. Phys., 2, 61-70.

Li, H., Dong, X., da Silva, E.B., de Oliveira, L.M., Chen, Y., Ma, L.Q., 2017 Mechanisms of metal sorption by biochars: Biochar characteristics and modifications. Chemosphere, 178, 466-478.

Li, Y., Wei, Y., Huang, S., Liu, X., Jin, Z., Zhang, M., Qu, J., Jin, Y., 2018 Biosorption of Cr(VI) onto *Auricularia auricula* dreg biochar modified by cationic surfactant: Characteristics and mechanism. J. Mol. Liq., 269, 824-832.

Lian, G., Wang, B., Lee, X., Li, L., Liu, T., Lyu, W., 2019 Enhanced removal of hexavalent chromium by engineered biochar composite fabricated from phosphogypsum and distillers grains. Sci. Total Environ., 697, 134119.

Liu, W., Ren, D., Wu, J., Wang, Z., Zhang, S., Zhang, X., Gong, X., 2020 Adsorption behavior of 2,4-DCP by rice straw biochar modified with CTAB. Environ. Technol., https://doi.org/10.1080/09593330.2020.1743367

Mandal, S., Sarkar, B., Bolan, N., Ok, Y.S., Naidu, R., 2017 Enhancement of chromate reduction in soils by surface modified biochar. J. Environ. Manage., 186, 277-284.

Mathurasa, L., Damrongsiri, S., 2017 Potential of using surfactants to enhance ammonium and nitrate adsorption on rice husk and its biochar. Appl. Environ. Res. 39, 11-22.

Mathurasa, L., Damrongsiri, S., 2018 Low cost and easy rice husk modification to efficiently enhance ammonium and nitrate adsorption. Int. J. Recycl. Org. Waste Agric., 7, 143-151.

Mehmood, K., Ahmad, H.R., Saifullah, 2019 Quantitative assessment of human health risk posed with chromium in waste, ground, and surface water in an industrial hub of Pakistan. Arab. J. Geosci., 12, 283.

Mi, X., Li, G., Zhu, W., Liu, L., 2016 Enhanced adsorption of orange II using cationic surfactant modified biochar pyrolyzed from cornstalk. J. Chem., 2016, Article ID 8457030, 7.

Mohan, D., Pittman, Jr., 2006 Activated carbons and low cost adsorbents for remediation of tri- and hexavalent chromium from water. J. Hazard. Mater., B137, 762-811.

Palansooriya, K.M., Shaheen, S.M., Chen, S.S., Tsang, D.C.W., Hashimoto, Y., Hou, D., Bolan, N.S., Rinklebe, J., 2020 Soil amendments for immobilization of potentially toxic elements in contaminated soils: A critical review. Environ. Int., 134, 105046.

PARC, 2020 Pakistan Agricultural Research Council. http://www.parc.gov.pk/index.php/en/csi/137-narc/crop-sciences-institue/728-groundnut

Patel, H., 2019 Fixed‑bed column adsorption study: a comprehensive review. Appl. Water Sci., 9, 45.

Puttamat, S., Pavarajarn, V., 2016 Adsorption study for removal of Mn(II) ion in aqueous solution by hydrated ferric(III) oxides. Int. J. Chem. Eng. Appl., 7, 239-243.

Qadir, A., Malik, R.N., Husain, S.Z., 2008 Spatio-temporal variations in water quality of Nullah Aik-tributary of the river Chenab, Pakistan. Environ. Monit. Assess., 140, 43-59.

Rafique, M.I., Usman, A.R.A., Ahmad, M., Sallam, A., Al-Wabel, M.I., 2020 In situ immobilization of Cr and its availability to maize plants in tannery waste–contaminated soil: effects of biochar feedstock and pyrolysis temperature. J. Soils Sediments, 20, 330-339.

Rajapaksha, A.U., Alam, M.S., Chen, N., Alessi, D.S., Igalavithana, A.D., Tsang, D.C.W., Ok, Y.S., 2018 Removal of hexavalent chromium in aqueous solutions using biochar: Chemical and spectroscopic investigations. Sci. Total Environ., 625, 1567-1573.

Rajapaksha, A.U., Chen, S.S., Tsang, D.C.W., Zhang, M., Vithanage, M., Mandal, S., Gao, B., Bolan, N.S., Ok, Y.S., 2016 Engineered/designer biochar for contaminant removal/immobilization from soil and water: Potential and implication of biochar modification. Chemosphere, 148, 276-291.

Rehman, S., Adnan, M., Iqbal, M., Nafees, M., 2017 Working efficiency of waste water treatment facility in Hayatabad industrial estates, Peshawar. J. Sci. Technol., 40, 41-52.

Riaz, U., Murtaza, G., Saifullah, Farooq, M., Aziz, H., Qasir, A.A., Mehdi, S.M., Qazi, M.A., 2020 Chemical fractionation and risk assessment of trace elements in sewage sludge generated from various states of Pakistan. Environ. Sci. Pollut. Res., https://doi.org/10.1007/s11356-020-07795-4

Sabur, M.A., Rahman, M.M., Safiullah, S., 2013 Treatment of tannery effluent by locally available commercial grade lime. J. Sci. Res. 5, 143-150.

Saleh, M.M., 2006 On the removal of cationic surfactants from dilute streams by granular charcoal. Water Res., 40, 1052-1060.

Soti, P.G., Jayachandran, K., Koptur, S., Volin, J.C., 2015 Effect of soil pH on growth, nutrient uptake, and mycorrhizal colonization in exotic invasive *Lygodium microphyllum*. Plant Ecol., 216, 989-998.

Sultan, H., Ahmed, N., Mubashir, M., Danish, S., 2020 Chemical production of acidified activated carbon and its influences on soil fertility comparative to thermo-pyrolyzed biochar. Sci. Rep., 10, 595. https://doi.org/10.1038/s41598-020-57535-4

Tan, C., Zeyu, Z., Sai, X., Hongtao, W., Wenjing, L., 2015 Adsorption behavior comparison of trivalent and hexavalent chromium on biochar derived from municipal sludge. Bioresour. Technol., 190, 388-394.

Torkashvand, A.M., Alidoust, M., Khomami, A.M., 2015 The reuse of peanut organic wastes as a growth medium for ornamental plants. Int. J. Recycl. Org. Waste Agricult., 4, 85-94.

Tran, H.N., You, S.J., Bandegharaei, A.H., Chao, H.P., 2017 Mistakes and inconsistencies regarding adsorption of contaminants from aqueous solutions: A critical review. Water Res., 120, 88-116.

Trivedy, R.K., Goel, P.K., Trisal, C.L., 1987 Practical methods in ecology and environmental science. Enviro Media Publications, pp 340.

US-EPA, 1992a Method 3005a Acid digestion of waters for total recoverable or dissolved metals for analysis by FLAA or ICP spectroscopy. United States Environmental Protection Agency.

US-EPA, 1992b Method 7196a Chromium, hexavalent (colorimetric). United States Environmental Protection Agency.

US-EPA, 1992c Method 3050 Acid digestion of sediments, sludges, and soils. United States Environmental Protection Agency.

US-EPA, 1992d Method 1311 Toxicity characteristic leaching procedure. United States Environmental Protection Agency.

US-EPA, 2014 Priority Pollutant List. United States Environmental Protection Agency.

Vithanage, M., Rajapaksha, A.U., Zhang, M., Thiele-Bruhn, S., Lee, S.S., Ok, Y.S., 2015 Acid-activated biochar increased sulfamethazine retention in soils. Environ. Sci. Pollut. Res., 22, 2175-2186.

Volesky, B., 2007 Biosorption and me. Water Res., 41, 4017-4029.

Wadhawan, S., Jain, A., Nayyar, J., Mehta, S.K., 2020 Role of nanomaterials as adsorbents in heavy metal ion removal from waste water: A review. J. Water Process Eng., 33, 101038.

Wang, C., Gu, L., Ge, S., Liu, X., Zhang, X., Chen, X., 2019 Remediation potential of immobilized bacterial consortium with biochar as carrier in pyrene-Cr(VI) co-contaminated soil. Environ. Technol., 40, 2345-2353.

Wang, H., Yang, N., Qiu, M., 2020 Adsorption of Cr(VI) from aqueous solution by biochar-clay derived from clay and peanut shell. J. Inorg. Mater., 35, 301-308.

Wang, L., Cho, D.W., Tsang, D.C.W., Cao, X., Hou, D., Shen, Z., Alessi, D.S., Ok, Y.S., Poon, C.S., 2019 Green remediation of As and Pb contaminated soil using cement-free clay-based stabilization/solidification. Environ. Int., 126, 336-345.

Wang, L., Ok, Y.S., Tsang, D.C.W., Alessi, D.S., Rinklebe, J., Wang, H., Masek, O., Hou, R., O'Connor, D., Hou, D., 2020 New trends in biochar pyrolysis and modification strategies: feedstock, pyrolysis conditions, sustainability concerns and implications for soil amendment. Soil Use Manag., 36, 358-386.

WHO. 2000. Global water supply and sanitation assessment 2000 report. World Health Organization.

Xia, S., Song, Z., Jeyakumar, P., Shaheen, S.M., Rinklebe, J., Ok, Y.S., Bolan, N., Wang, H., 2019 A critical review on bioremediation technologies for Cr(VI)-contaminated soils and wastewater. Crit. Rev. Env. Sci., 49, 1027-1078.

Xu, D., Gao, Y., Lin, Z., Gao, W., Zhang, H., Karnowo, K., Hu, X., Sun, H., Hassan, S.S.A.S., Zhang, S., 2019 Application of biochar derived from pyrolysis of waste fiberboard on tetracycline adsorption in aqueous solution. Front. Chem., 7:943. doi: 10.3389/fchem.2019.00943

Yang, X., Wan, Y., Zheng, Y., He, F., Yu, Z., Huang, J., Wang, H., Ok, Y.S., Jiang, Y., Gao, B., 2019 Surface functional groups of carbon-based adsorbents and their roles in the removal of heavy metals from aqueous solutions: A critical review. Chem. Eng. J., 366, 608-621.

Zhang, A., Li, X., Xing, J., Xu, G., 2020 Adsorption of potentially toxic elements in water by modified biochar: A review. J. Environ. Chem. Eng., 8, 104196.

Zhang, M., Ahmad, M., Al-Wabel, M.I., Vithanage, M., Rajapaksha, A.U., Kim, H.S., Lee, S.S., Ok, Y.S., 2015 Adsorptive removal of trichloroethylene in water by crop residue biochars pyrolyzed at contrasting temperatures: continuous fixed-bed experiments. J. Chem. 2015. Article ID 647072, 6.

Zhou, L., Xu, D., Li, Y., Pan, Q., Wang, J., Xue, L., Howard, A., 2019 Phosphorus and nitrogen adsorption capacities of biochars derived from feedstocks at different pyrolysis temperatures. Water, 2019, 11, 1559.

Zibaei, Z., Fasaei, R.G., Ronaghi, A., Zarei, M., Zeinali, S., Improvement of biochar capability in Cr immobilization via modification with chitosan and hematite and inoculation with *Pseudomonas putida*. Commun. Soil Sci. Plant Anal., 51, 963-975.

List of Tables

List of Figures

Table 1: Parameters of different adsorption isotherm models (a) and kinetic models (b) for the removal of Cr(VI) from water by the pristine biochar (PBC) and the engineered biochar (EBC).

(a)

Biochar/ isotherm model	Langmuir				Freundlich				Temkin			
	R^2	χ^2	Q_{max} (mg g^{-1})	K_L (L g^{-1})	R^2	χ^2	N	K_F (mg g^{-1})	R^2	χ^2	B	A
PBC	0.998	0.073	14.56	0.006	0.986	0.423	0.699	0.194	0.914	0.200	577.5	0.181
EBC	0.978	0.700	27.05	0.009	0.964	1.196	0.696	0.491	0.818	0.519	371.1	0.403

(b)

Biochar/ kinetic model	First order			Second order			Pseudo-second order					Intra-particle diffusion			
	R^2	χ^2	k_1 (g mg^{-1} h^{-1})	R^2	χ^2	k_2 (g mg^{-1} h^{-1})	R^2	χ^2	q_e (mg g^{-1})	k_2' (g mg^{-1} h^{-1})	h (mg g^{-1} h^{-1})	R^2	χ^2	K_d (mg g^{-1})	C
PBC	0.891	0.031	0.011	0.859	0.104	-0.030	0.985	10.351	0.497	1.020	0.252	0.835	0.022	0.031	0.261
EBC	0.836	0.089	0.008	0.810	0.047	-0.012	0.996	2.360	0.851	1.088	0.788	0.877	0.016	0.045	0.542

Table 2: (a) Adsorption process parameters and Thomas model parameters for Cr(VI) adsorption and (b) desorption process parameters for Cr(VI) desorption for the pristine biochar (PBC) and the engineered biochar (EBC) in continuous fixed-bed columns.

(a)

Biochar	Sorption process		Thomas model		
	Removal (%)	q_{eq} (mg g^{-1})	k (mL min^{-1} mg^{-1})	q_o (mg g^{-1})	R^2
PBC	60.42	18.54	0.048	3.28	0.462
EBC	74.72	22.93	0.072	2.03	0.667

(b)

Biochar	Desorbed Cr(VI) (mg g^{-1})	Column elution efficiency (%)
PBC	13.83	74.61
EBC	10.45	45.56

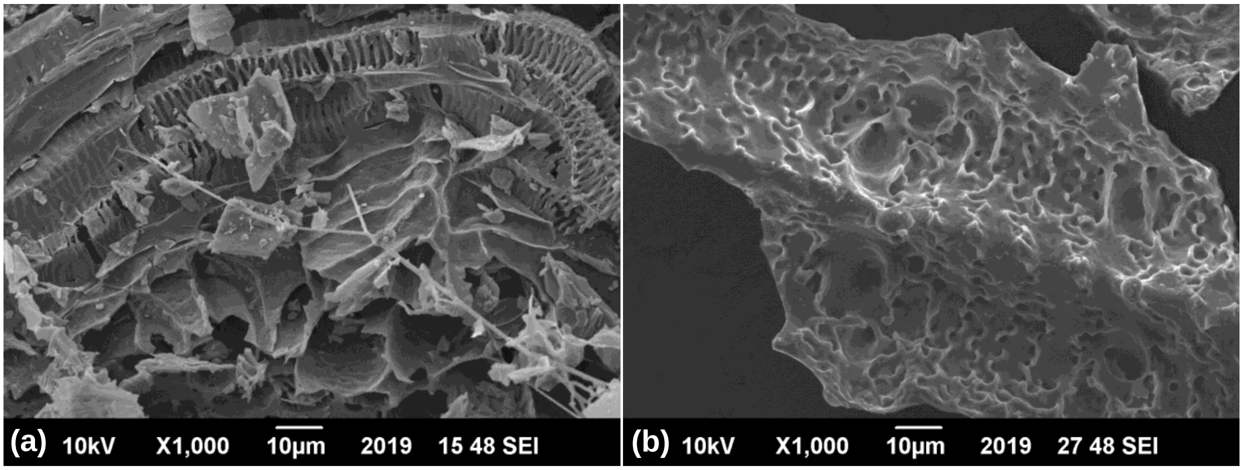

Fig. 1: The SEM images of (a) the pristine biochar (PBC) and (b) the engineered biochar (EBC).

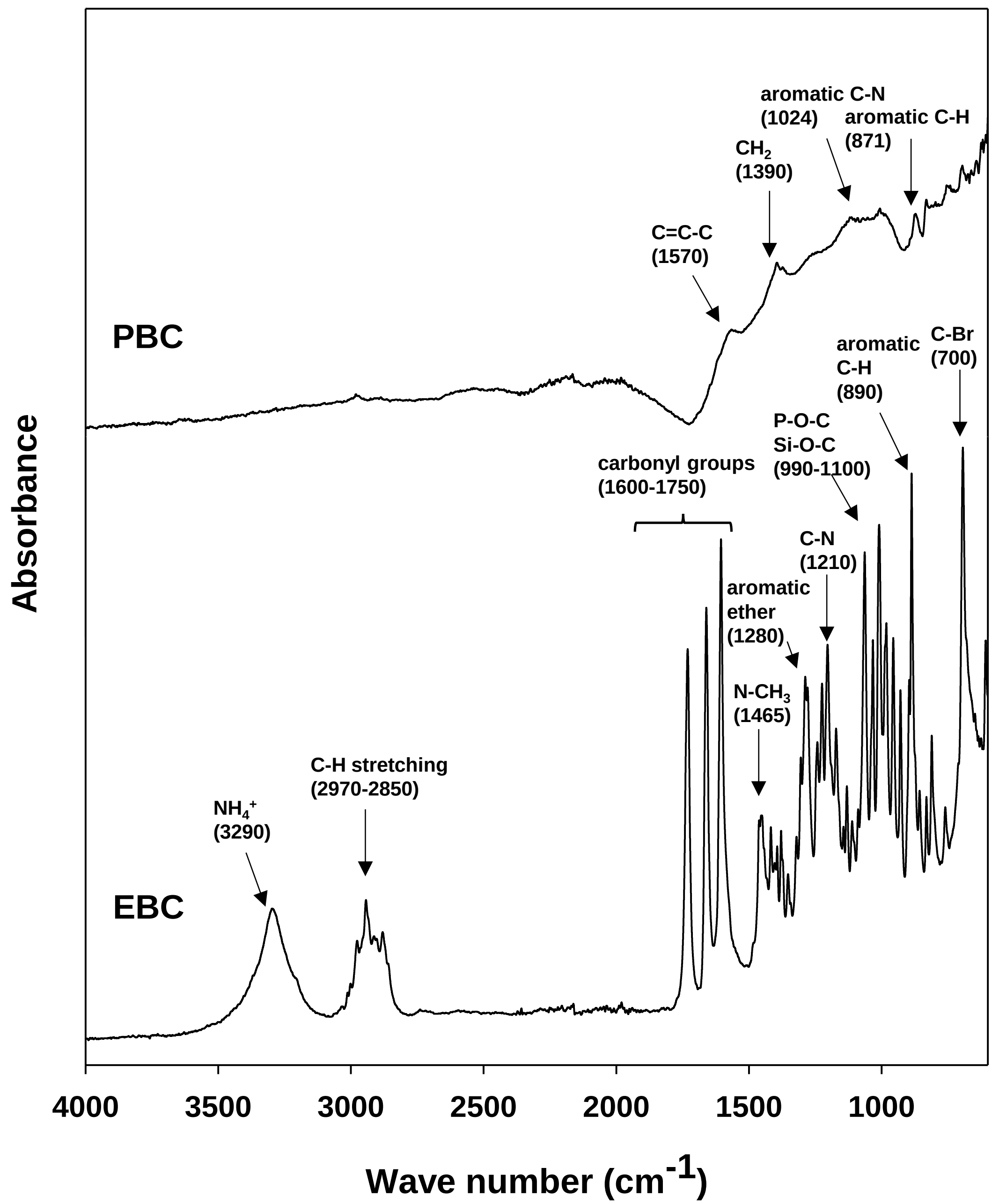

Fig. 2: The FTIR spectra of the pristine biochar (PBC) and the engineered biochar (EBC).

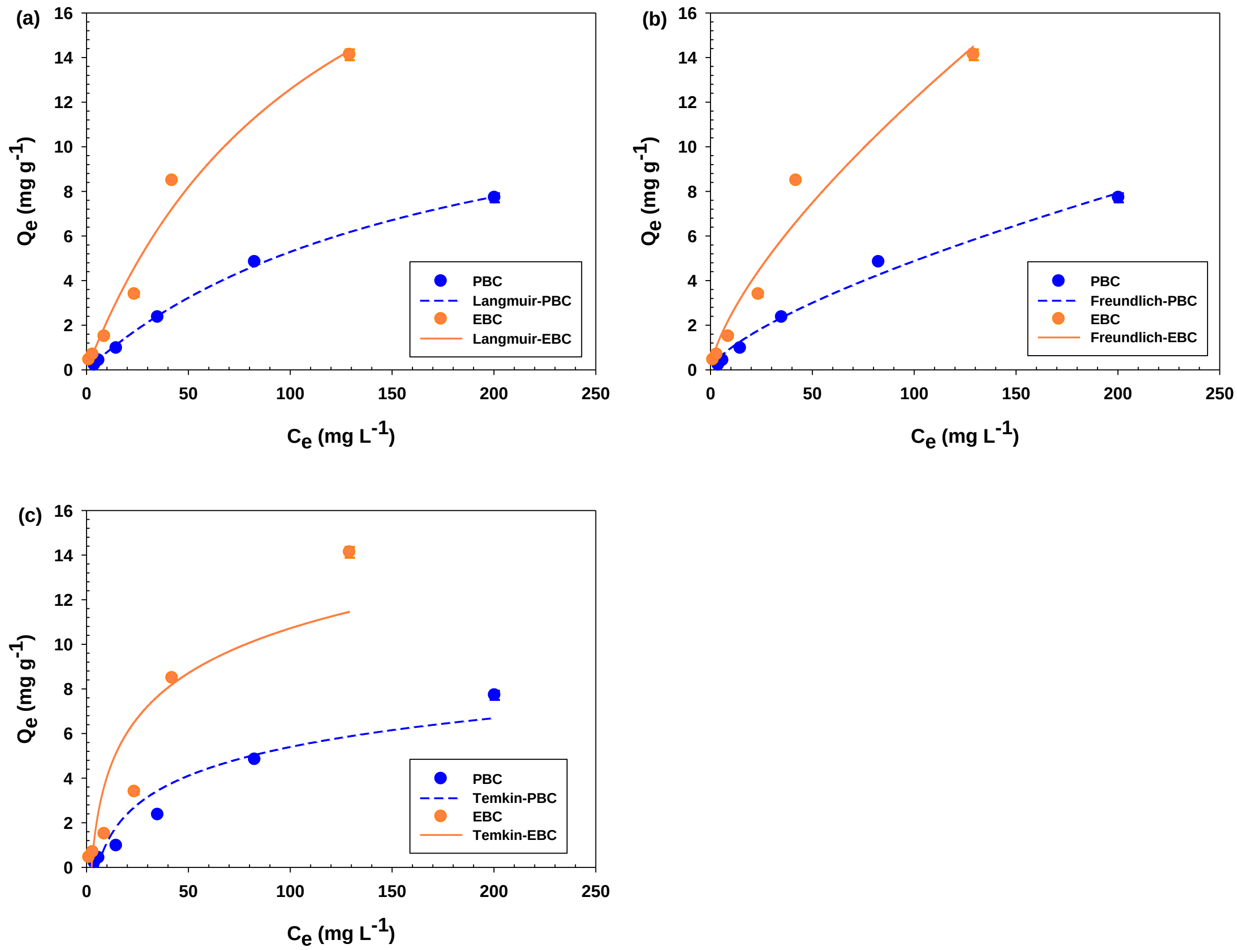

Fig. 3: Non-linear fittings of the (a) Langmuir, (b) Freundlich, and (c) Temkin isotherm models to the experimental data of Cr(VI) adsorption onto the pristine biochar (PBC) and the engineered biochar (EBC).

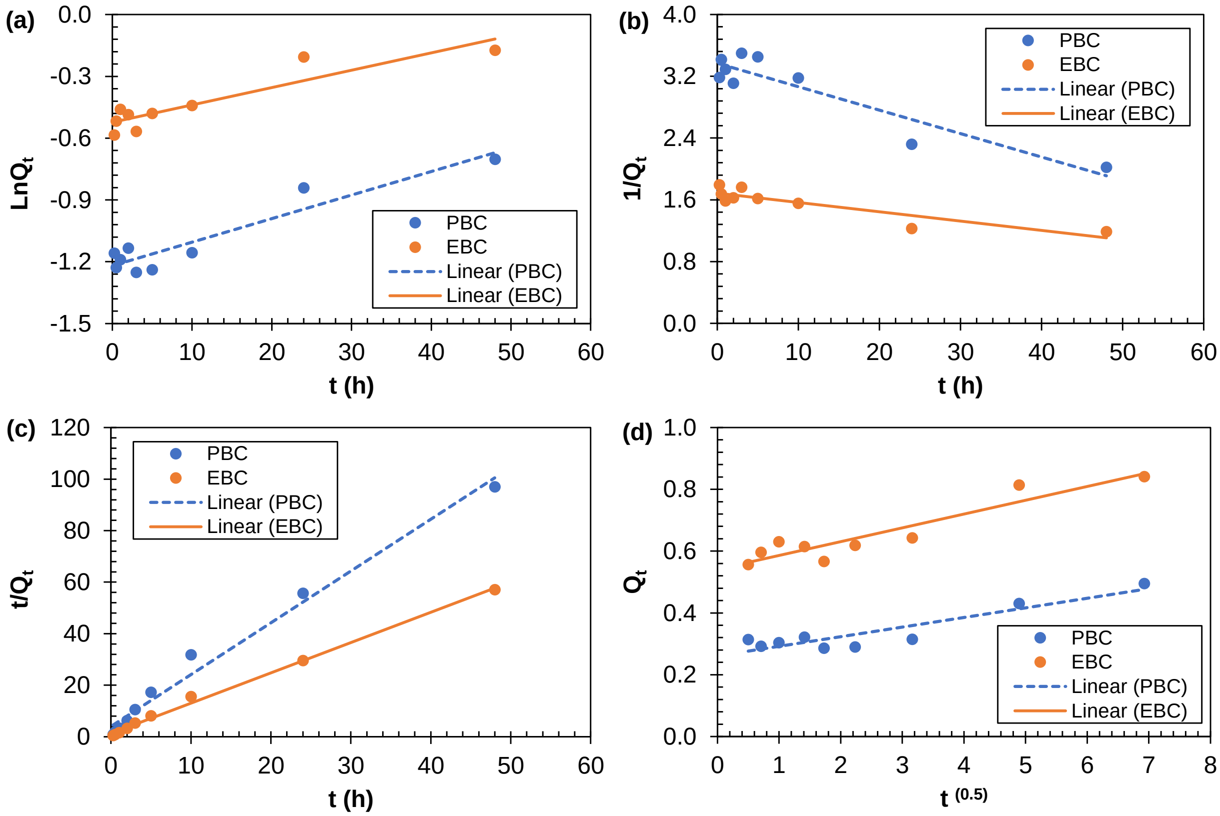

Fig. 4: Linear fittings of the (a) first-order, (b) second-order, (c) pseudo-second order, and (d) intra-particle diffusion kinetic models to the experimental data of Cr(VI) adsorption onto the pristine biochar (PBC) and the engineered biochar (EBC).

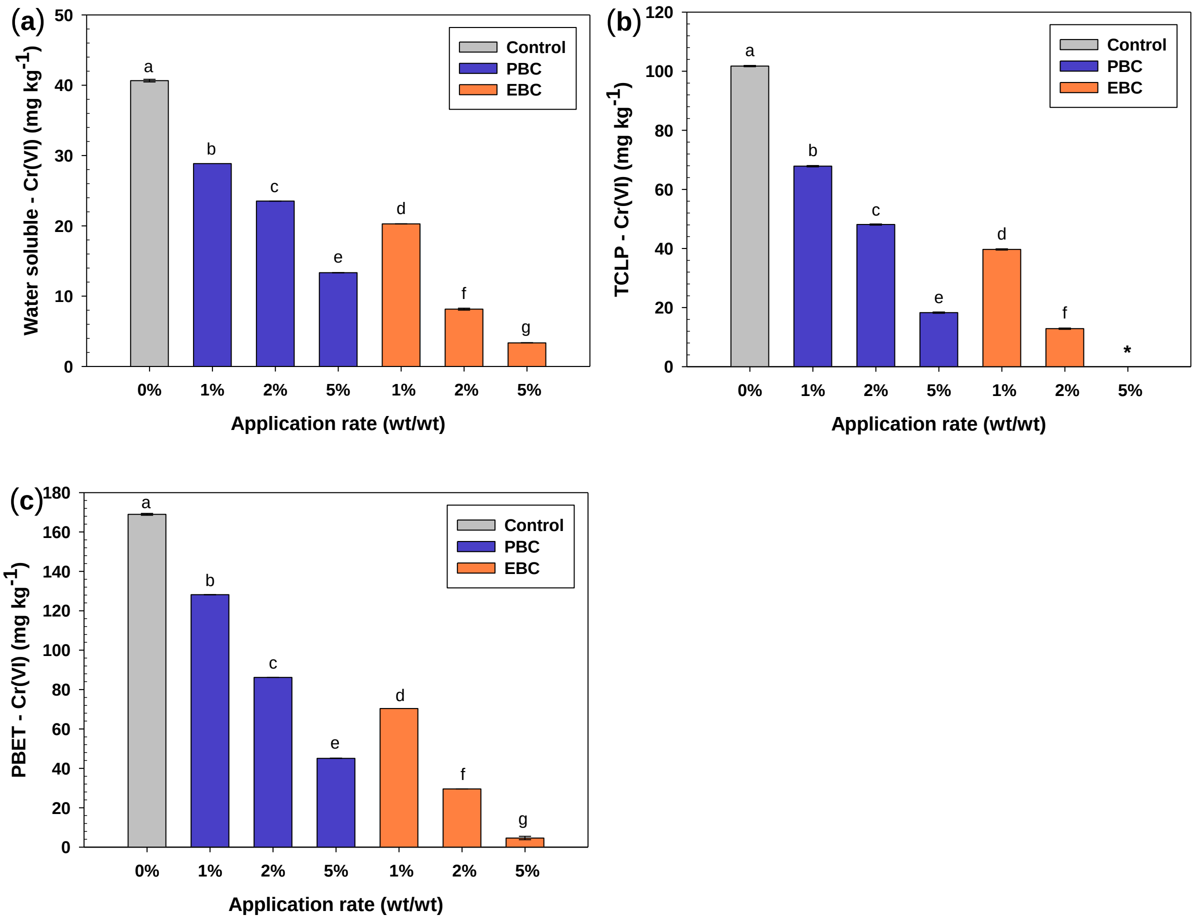

Fig. 5: Effect of various application rates of the pristine biochar (PBC) and the engineered biochar (EBC) on (a) water, (b) TCLP, and (c) PBET extracted Cr(VI) in contaminated soil. The similar letters on each bar indicate non-significant differences between the different treatments at $P < 0.05$ (* = not detected).

Supplementary material

A Remediation Approach to Chromium-Contaminated Water and Soil using Engineered Biochar Derived from Peanut Shell

Hafiza Afia Murad[a,1], Mahtab Ahmad[a,1]*, Jochen Bundschuh[b], Yohey Hashimoto[c], Ming Zhang[d], Binoy Sarkar[e], Yong Sik Ok[f,*]

[a] Department of Environmental Sciences, Faculty of Biological Sciences, Quaid-i-Azam University, Islamabad 45320, Pakistan

[b] UNESCO Chair on Groundwater Arsenic within the 2030 Agenda for Sustainable Development, University of Southern Queensland, West Street, Toowoomba, Queensland 4350, Australia

[c] Department of Bio-Applications and Systems Engineering, Tokyo University of Agriculture and Technology, 2-24-16 Koganei, Tokyo 184-8588, Japan

[d] Department of Environmental Engineering, China Jiliang University, No. 258 Xueyuan Street, Hangzhou, Zhejiang 310018, China

[e] Lancaster Environment Center, Lancaster University, Lancaster, LA1 4YQ, United Kingdom

[f] Korea Biochar Research Center, APRU Sustainable Waste Management Program & Division of Environmental Science and Ecological Engineering, Korea University, Seoul, Korea

[1] These authors share co-first authorship.

* Corresponding authors

Email: mahmad@qau.edu.pk (Mahtab Ahmad); yongsikok@korea.ac.kr (Yong Sik Ok)

Analysis of column data

The total adsorbed quantity of Cr(VI) (q_{total}) was calculated from the following equation:

$$q_{total} = \frac{QA}{1000} = \frac{Q}{1000} \int C_{ad}\, dt$$

where *Q* is the flow rate (mL min^{-1}) of wastewater; *A* is the area under the curve, which was calculated through the integration of the plot of C_{ad} (adsorbed Cr(VI) concentration) versus *t* time (min). The total amount of Cr(VI) sent to column (M_{total}) was calculated from the following equation:

$$M_{total} = \frac{C_o\, Q\, t_{total}}{1000}$$

where C_o is the initial Cr(VI) concentration (mg L^{-1}) fed to the column, and t_{total} is the total flow time (min).

The following equation was used to evaluate the column performance:

$$\text{Removal } (\%) = \frac{q_{total}}{M_{total}} \times 1000$$

The column capacity or equilibrium Cr(VI) sorption (q_{eq}) was calculated from the following equation:

$$q_{eq} = \frac{q_{total}}{X}$$

where q_{total} is the total amount of Cr(VI) adsorbed in the column and *X* is the adsorbent amount (g) filled in the column.

Table S1: Selected properties of the experimental soil.

Parameter	Values
pH	5.00 ± 0.02
Electrical conductivity (dS m^{-1})	0.081± 0.00
Texture	Silt loam
Clay (%)	25.32 %
Silt (%)	53.98 %
Sand (%)	20.64 %
Organic matter (%)	0.93 ± 0.003
Water soluble phosphate (mg kg^{-1})	62.00 ± 0.71
Water soluble nitrates (mg kg^{-1})	26.33 ± 0.98
Total Cr (mg kg^{-1})	1992.23 ± 19.20
Cr(VI) (mg kg^{-1})	212.88 ± 15.06

Table S2: Proximate analysis and physicochemical parameters of the pristine biochar (PBC) and the engineered biochar (EBC).

Parameter	Values	
	PBC	EBC
Moisture (%)	3.34 ± 0.19^{a}	2.49 ± 2.44^{b}
Mobile matter (%)	24.11 ± 0.56^{a}	20.15 ± 0.35^{b}
Resident matter (%)	15.13 ± 2.29^{a}	16.13 ± 12.2^{a}
Ash (%)	57.42 ± 1.93^{a}	59.63 ± 4.31^{a}
pH	9.46 ± 0.01^{a}	6.30 ± 0.01^{b}
pH_{PZC}	7.44 ± 0.07^{a}	6.70 ± 0.04^{b}
Electrical conductivity (dS m^{-1})	0.249 ± 0.007^{a}	0.149 ± 0.002^{b}
Organic matter (%)	1.66 ± 0.33^{a}	1.15 ± 0.34^{b}

The similar upper case letters on the values indicate non-significant differences at $P < 0.05$ between the two biochars.

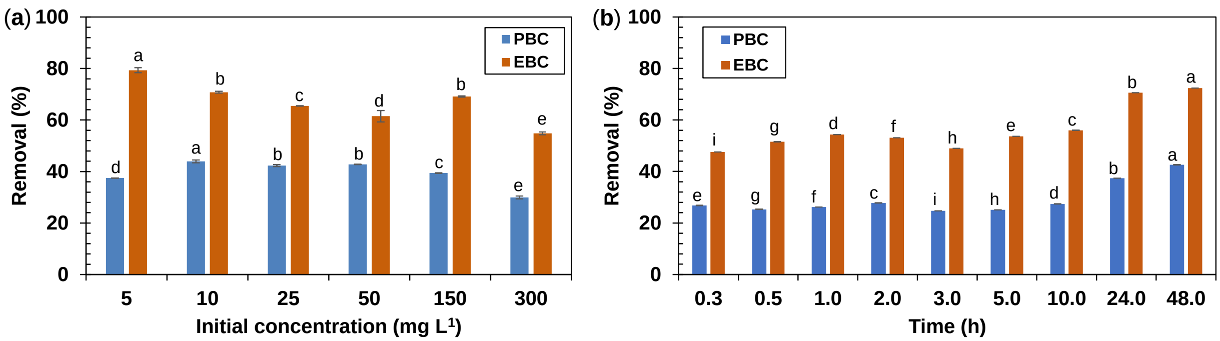

Fig. S1: Effect of (a) initial concentration and (b) contact time on percentage removal of Cr(VI) from water by the pristine biochar (PBC) and the engineered biochar (EBC). The similar letters on the bars indicate non-significant differences at $P < 0.05$.

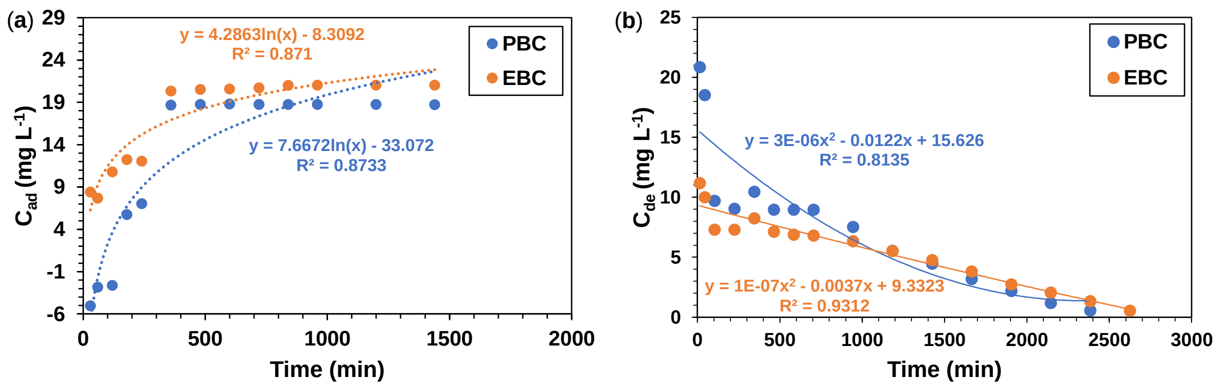

Fig. S2: (a) Adsorbed and (b) desorbed concentration of Cr(VI) as a function of time in a continuous fixed-bed column of the pristine biochar (PBC) and the engineered biochar (EBC).

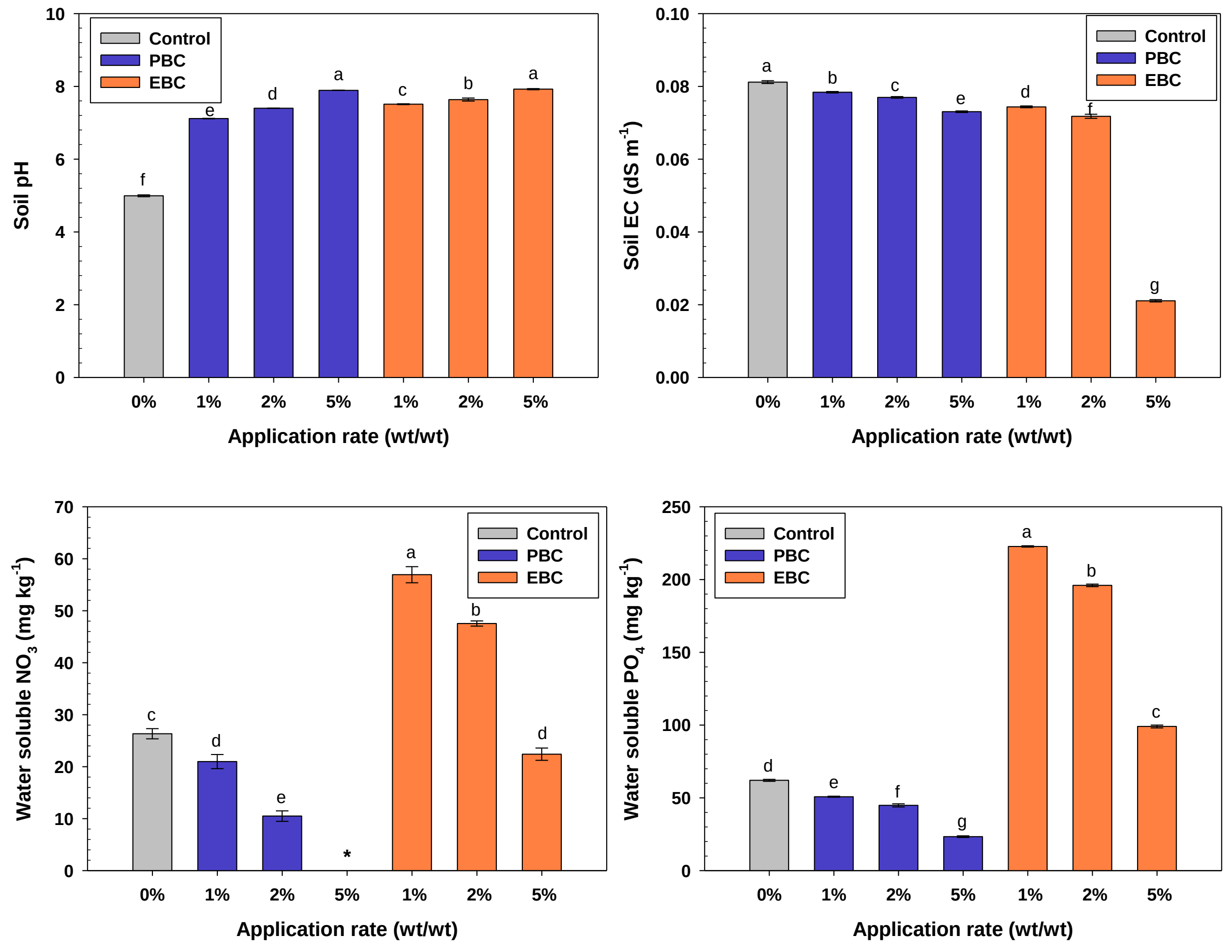

Fig. S3: Effect of various application rates of the pristine biochar (PBC) and the engineered biochar (EBC) on (a) soil pH, (b) soil EC, (c) water-soluble nitrates, and (d) water-soluble phosphates. The similar letters on each bar indicate non-significant differences between the different treatments at P <0.05.